



Estimation of thermal properties of fuzzy carbon fiber heat exchanger using micromechanics approach

Rahul Sharma^a, Vivek Kumar Gaba^a, S. I. Kundalwal^b and R. Suresh Kumar^{*a}

^aDepartment of Mechanical Engineering, National Institute of Technology Raipur, Raipur-492 010, Chhattisgarh, India

^bDepartment of Mechanical Engineering, Indian Institute of Technology Indore, Indore-453 552, Madhya Pradesh, India

E-mail: rskumar.me@nitrr.ac.in

Manuscript received online 28 March 2020, accepted 15 June 2020

Effect of straight radially grown carbon nanotubes (CNTs) on the periphery of a hollow cylindrical fiber (HCF) has been considered for the thermal conductivity estimation of the proposed fiber. Such a hollow fiber with the presence of CNTs on the periphery is termed as fuzzy fiber heat exchanger (FFHE). Two micromechanics approaches namely method of cells (MOC) and the effective medium (EM) have been employed in thermal conductivity estimation of the carbon FFHE. The presence of CNTs radially on the outer periphery of the hollow base fiber tend to significantly improve the transverse thermal conductivities (out-of-plane) of carbon FFHE in comparison with hollow carbon fiber (i.e, without CNTs). Approximately an improvement in transverse thermal conductivities of over 400% is seen in FFHE in the presence of only few percentages of radially grown CNTs. Also, it is observed that thermal interfacial resistance between CNT/polymer matrix has negligible or zero effect affect in the estimated thermal properties of FFHE.

Keywords: Fuzzy fiber heat exchanger (FFHE), method of cells (MOC), effective medium (EM) approach, carbon nanotubes (CNTs), micromechanics.

Introduction

The superiority of CNTs¹ has indeed opened the doors for great deal of research pertaining to the improvement in the properties (mechanical and thermal) of the same. The research in this area during the past years has unequivocally shown the terapascal range of Young's modulus of CNTs along the axis of the CNT (single-walled CNTs)²⁻⁴. Also, the thermal conductivity of single-walled CNTs are greater than that of the diamond and multi-walled CNTs⁵⁻⁸. Hence to harness the exceptional thermal conductivities of CNTs, research on the usage of the same for the development of reinforced composites embedded with the CNTs. For example, Choi *et al.*⁹ used nanotube suspended in oil and measures the corresponding thermal conductivity in a two-step process. The measurements show higher thermal conductivities compared with the theoretical calculations of the same. Biercuk *et al.*¹⁰ fabricated CNT-reinforced composites and observed the enhancement in the conductivity of 125% at 1 wt% CNT load-

ing. Guthy *et al.*¹¹ coagulated the CNT/PMMA with 6% CNT loading and an enhancement of 240% of the thermal conductivity. Nan *et al.*¹² found remarkable enhancement in the conductivity of nanocomposites with little amounts of dispersions of the CNTs. The CNT/polymer thermal interfacial resistance (R_k) also called as the Kapitza resistance occurs due to the properties mismatch. Wilson *et al.*¹³ reported the range of values of R_k between the type of nano particle and the polymer given by $0.77 \times 10^{-8} \text{ m}^2\text{K/W}$ to $20 \times 10^{-8} \text{ m}^2\text{K/W}$. Huxtable *et al.*¹⁴ found about $8.3 \times 10^{-8} \text{ m}^2\text{K/W}$ thermal interfacial resistance between the CNT/matrix. Nan *et al.*¹⁵ incorporated the findings of Huxtable *et al.*¹⁴ and determined the conductivities of composite reinforced with CNTs using effective medium (EM) approach. They also found that the higher values of CNT/matrix resistance degrades the conductivities drastically. Thereafter many researchers predicted the thermal properties of nanocomposites considering the thermal interfacial resistance between CNT/polymer¹⁶⁻¹⁹.

However, research further is now focused upon enhancing the transverse properties (out-of-plane) of multifunctional material composites containing short CNTs^{20–22}. Veedu *et al.*²³ found the significant improvement in properties of composites composed of CNTs of multi-walled type on the periphery of base fibers. The test carried out by them reveal significant improvement in conductivities in the thickness (i.e. transverse) direction of the base fiber. Using the electrophoresis technique the single- or the multi-walled CNTs are selectively deposited on the base carbon fibers by Bekyarova *et al.*²⁴. The results of the study show that selective deposition of single-walled CNT on the base fiber enhances the interlayer shear strength to approximately ~30% while the out-of-plane electrical conductivities are doubled in comparison with the base fibers having no CNTs. Yamamoto *et al.*²⁵ developed a hybrid composite with aligned CNTs deposited on the woven fibers and by loading 2.2% CNTs doubles the thermal conductivities of the base composite. Carbon/carbon composite developed by Chen *et al.*²⁶ augmented by CNTs on the periphery of the base fiber (i.e. carbon). They found conductivity of the carbon/carbon composite higher in comparison with the composite containing no CNTs. Fibers coated with CNTs on their periphery are termed as “fuzzy fibers”^{25,28,29}.

In applications of high heat buildups like the heat engines and electric mother boards where dissipation of heat quickly is a challenging task which can be accomplished by addition of advanced CNT-reinforced layers. Hollow cylindrical fiber (HCF) made of carbon material acts as a heat exchanger element in many technological applications. Application of the polymer matrix reinforced with the CNTs on the periphery of HCF may enhance the heat dissipation across the thickness of the same. Unlike external metal layer that adds weight, the CNT-reinforced polymer matrix layer can enhance multifunctional properties of the HCF heat exchanger with minimum weight. Such HCF heat exchanger coated with the CNT-reinforced polymer matrix layer is termed as fuzzy fiber heat exchanger (FFHE). However, the thermal conductivities of such FFHE has not been reported yet. The present study hence is devoted in this direction of estimation the thermal properties of FFHE. The study also focusses on investigating the thermal interfacial resistance of CNT/polymer effect on the same.

Architecture of FFHE:

Fig. 1 represents the schematic illustration of carbon

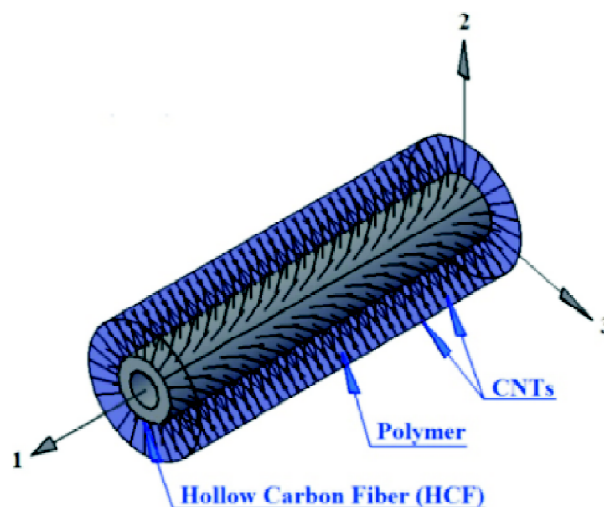


Fig. 1. Diagrammatic representation of carbon FFHE.

FFHE considered for the present study. As shown in the figure, the straight CNTs are grown radially and are distributed uniformly on the periphery of the HCF. These CNTs surrounding the HCF are in itself act as reinforcements in the matrix material around the HCF in the transverse direction. This material when observed depict a conventional heat exchanger and hence the name FFHE is subtle. The HCF is further embedded as reinforcement in the surrounding CNT/polymer material called the PMNC (polymer matrix nano com-

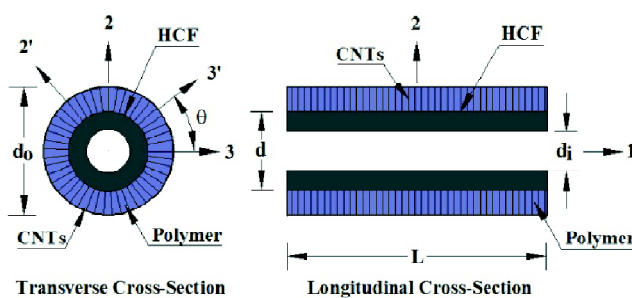


Fig. 2. FFHE cross-sections.

posite). The sectional views of FFHE is depicted in Fig. 2 schematically.

FFHE thermal conductivity estimation using micromechanics approaches:

This segment details the adopted micromechanical methods viz. the method of cells (MOC) and the effective medium

(EM) approaches for estimating the thermal conductivities of different constituents. First step in this direction is to estimate the PMNC material properties and subsequently embedding the PMNC matrix material with reinforcements as HCF, the FFHE conductivities are evaluated. Fig. 3 illustrate the step wise procedure involved in the computations of FFHE conductivities and the details regarding the same are as follows:

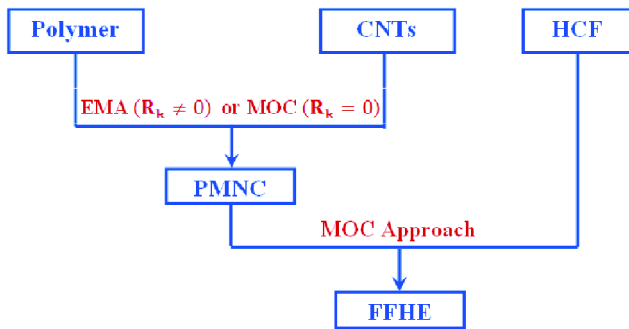


Fig. 3. Micromechanical modelling steps.

Step 1: PMNC conductivities are estimated first using either of the above mentioned approaches. The thermal interfacial resistance is zero when MOC approach ($R_k \neq 0$) is used while the same is non zero when the EM approach is used for the evaluations of the same.

Step 2: PMNC conductivities determined in Step 1 are considered along with the HCF whose thermal conductivity is known priori. Employing MOC approach and making use of the above values, the final FFHE conductivities are predicted.

Method of cells approach:

MOC is a micromechanics approach and the adoption procedure for the estimation of thermal conductivity of PMNC and FFHE enlisted here.

The initial MOC approach by Aboudi²⁹ has been reformed suiting the present analysis for predicting the PMNC material conductivity in the unwound form. Fig. 2 shows the FFHE where it is seen that HCF is surrounded by the PMNC material on the periphery in the wound form. As shown in Fig. 4, the CNTs are along direction-3 reinforced in the unwound PMNC. Therefore unwound PMNC material conductivities estimated using the MOC are approximately same as those

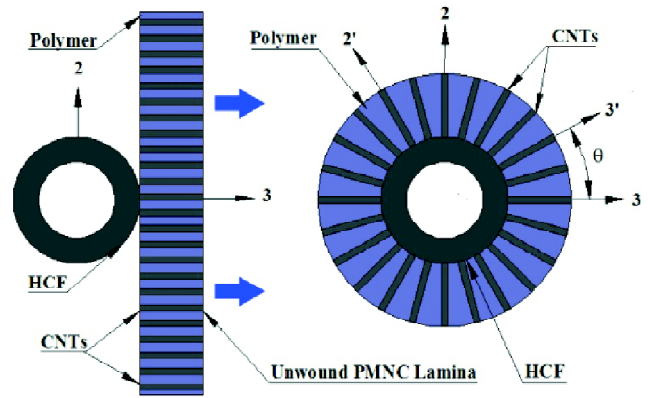


Fig. 4. Section side view of FFHE with PMNC (unwound and wound).

in the wound form over the HCF. Thus FFHE thermal conductivity predictions starts with the estimations of the same for the unwound lamina (K_i^{nc}). As mentioned in the previous section the CNTs are considered as solid continua in the fiber form^{11,12,15-19} that are spaced in polymer matrix uniformly. Such CNTs are aligned in transverse direction of HCF along the 3-axis. The PMNC in the unwound form is depicted as a double periodic array of cells in directions along x_1 - and x_2 -, respectively. The repeating unit cell (RUC) contains four subcell as shown in Fig. 5. The labelling of each subcell is done by β, γ each denoting the subcell locations in the respective x_1 - and the x_2 -directions. The material of the subcell can be any of these (CNT reinforcements or polymer ma-

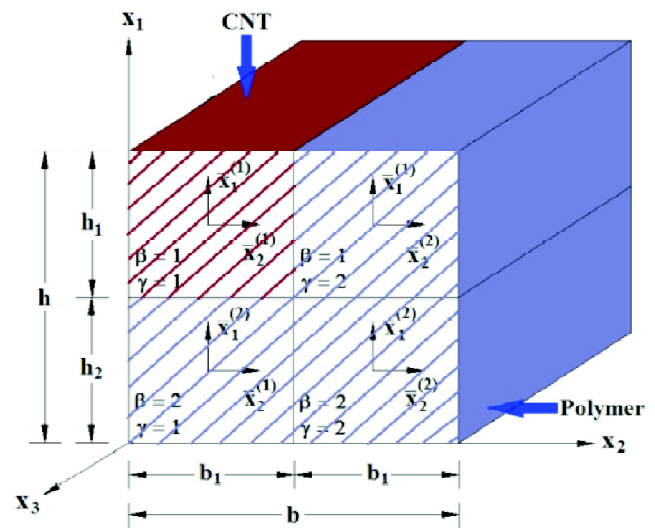


Fig. 5. Unit cell representation of PMNC with four sub cells ($\beta, \gamma = 1, 2$).

trix). Introducing the local coordinate systems ($\bar{x}_1^{(\beta)}$, ($\bar{x}_2^{(\gamma)}$ and x_3) whose origins lie at the each cell centroids. The temperature deviation using MOC approach from the reference point T_R representing the stress and strain free surfaces is $\Delta\Theta^{(\beta\gamma)}$ and in the expanded form given by

$$\Delta\Theta^{(\beta\gamma)} = \Delta T + \bar{x}_1^{(\beta)} \xi_1^{(\beta\gamma)} + \bar{x}_2^{(\gamma)} \xi_2^{(\beta\gamma)} \quad (1)$$

with $\xi_1^{(\beta\gamma)}$ and $\xi_2^{(\beta\gamma)}$ characterize the temperature dependence as functions of local coordinates. Each subcell volume is represented by ($V_{\beta\gamma}$) and given by

$$V_{\beta\gamma} = b_\beta h_\gamma L \quad (2)$$

where L , b_β , and h_γ are the subcells length, width and height while the RUC volume (V) is given by

$$V = bhL \quad (3)$$

To maintain the consistency of smooth transfer of properties, temperature continuity at the interfaces of the subcell are considered which results in the following

$$h_1 \xi_1^{(1\gamma)} + h_2 \xi_1^{(2\gamma)} = (h_1 + h_2) \frac{\partial T}{\partial x_1}$$

$$b_1 \xi_2^{(\beta 1)} + b_2 \xi_2^{(\beta 2)} = (b_1 + b_2) \frac{\partial T}{\partial x_2} \quad (4)$$

While average heat flux in the subcell:

$$\bar{q}_1^{(\beta\gamma)} = -K_1^{(\beta\gamma)} \frac{\partial T}{\partial x_1}, \quad \bar{q}_2^{(\beta\gamma)} = -K_2^{(\beta\gamma)} \frac{\partial T}{\partial x_2}$$

$$\bar{q}_3^{(\beta\gamma)} = -K_3^{(\beta\gamma)} \frac{\partial T}{\partial x_3} \quad (5)$$

where $K_i^{(\beta\gamma)}$ denotes the corresponding subcell conductivities.

The heat flux average of the PMNC material in the unwound form is given by

$$q_i = \frac{1}{V} \sum_{\beta,\gamma=1}^2 V_{\beta\gamma} \bar{q}_i^{(\beta\gamma)} \quad (6)$$

while conditions of continuity at the subcell interfaces results in

$$\bar{q}_1^{(1\gamma)} = \bar{q}_1^{(2\gamma)}, \quad \bar{q}_2^{(\beta 1)} = \bar{q}_2^{(\beta 2)} \quad (7)$$

The heat flux averages in terms of temperature gradients and the PMNC thermal conductivity (K_i^{nc}) are as follows:

$$\bar{q}_1 = -K_1^{nc} \frac{\partial T}{\partial x_1}, \quad \bar{q}_2 = -K_2^{nc} \frac{\partial T}{\partial x_2}$$

$$\bar{q}_3 = -K_3^{nc} \frac{\partial T}{\partial x_3} \quad (8)$$

Eliminating the micro variables $\xi_1^{(\beta\gamma)}$ and $\xi_2^{(\beta\gamma)}$, and employing the interface continuity, the PMNC thermal conductivity in the unwound form are given as³⁰:

$$K_1^{nc} = \frac{K^p \left\{ K^n [h(V_{11} + V_{21}) + h_2(V_{12} + V_{22})] \right\}}{hbL(K^p h_1 + K^n h_2)}$$

$$K_2^{nc} = \frac{K^p \left\{ K^n [b(V_{11} + V_{12}) + b_2(V_{21} + V_{22})] \right\}}{hbL(K^p b_1 + K^n b_2)}$$

$$K_3^{nc} = \frac{K^n V_{11} + K^p (V_{12n} + V_{21} + V_{22})}{hbL} \quad (9)$$

The superscripts found in eq. (9) have their usual meaning 'nc' for PMNC, 'n' for CNT and 'p' for the polymer matrix. The conductivities of PMNC given in eq. (9) may also be represented in matrix form given by:

$$[K^{nc}] = \begin{bmatrix} K_1^{nc} & 0 & 0 \\ 0 & K_2^{nc} & 0 \\ 0 & 0 & K_3^{nc} \end{bmatrix} \quad (10)$$

The entries of the matrix directly provides the information of thermal conductivities of PMNC wound round the HCF when the CNTs are aligned along 3-axis. In order to determine the orientation effect of CNTs in the 2-3 plane inclined at θ with the 3-axis on the thermal conductivities of the PMNC, eq. (10) provides the same in the (1', 2', 3') coordinate system. They are then transformed in respect of 1-2-3 coordinate system by the use of planar transformation matrix multiplication³¹:

$$[\bar{K}^{PMNC}] = [T]^{-T} [K^{nc}] [T]^{-1} \quad (11)$$

in which

$$[T] = \begin{bmatrix} 1 & 0 & 0 \\ 0 & \cos\theta & -\sin\theta \\ 0 & \sin\theta & \cos\theta \end{bmatrix}$$

Therefore, the choice of the material coordinate plays a significant role in finding the PMNC conductivities and hence the same may effect overall conductivities of FFHE. By adopting a homogenization technique on the RVE of the annular section of PMNC, the effective thermal properties may be computed in the PMNC phase^{30,31}. These RVEs may prove to be very effective in the estimation of overall conductivities of PMNC by adopting the volume averaging technique. Thermal conductivities of PMNC in 1-2-3 material coordinate of the FFHE are given by³¹

$$[K^{PMNC}] = \frac{1}{\pi(R^2 - a^2)} \int_0^{2\pi} \int_a^R [\bar{K}^{PMNC}] r dr d\theta \quad (12)$$

the estimated conductivities $[K^{PMNC}]$ of the PMNC are transverse isotropic nature. Hence, considering the same nature, the MOC approach is used to estimate the conductivities (K_i) of FFHE with HCF as reinforcement is aligned along 1-direction and given by:

$$K_1 = \frac{K^f V_{11} + K_1^{PMNC} (V_{12} + V_{21} + V_{22})}{hbL}$$

$$K_2 = \frac{K_2^{PMNC} \left\{ K^f [h(V_{11} + V_{21}) + h_2(V_{12} + V_{22})] + K_2^{PMNC} h_1(V_{12} + V_{22}) \right\}}{hbL(K_2^{PMNC} h_1 + K^f h_2)}$$

$$K_3 = \frac{K_3^{PMNC} \left\{ K^f [b(V_{11} + V_{12}) + b_2(V_{21} + V_{22})] + K_3^{PMNC} b_1(V_{21} + V_{22}) \right\}}{hbL(K_3^{PMNC} b_1 + K^f b_2)} \quad (13)$$

Effective medium approach (EMA):

The Maxwell-Garnett type EM micromechanical approach is adopted for the prediction of PMNC thermal conductivity accounting R_k ($R_k \neq 0$) of the CNT/polymer. The consistent assumption of CNTs as solid continua^{11,12,15-19}, the EM micromechanics approach given by Nan *et al.*³² is revised to predict the PMNC (unwound) thermal conductivities (K_i^{nc}) containing CNTs and the same are given as follows³³.

$$K_1^{nc} = K_2^{nc} = K^p \frac{K^n(1 + \alpha) + K^p + v_n[K^n(1 - \alpha) - K^p]}{K^n(1 + \alpha) + K^p - v_n[K^n(1 - \alpha) - K^p]}$$

$$K_3^{nc} = v_n K^n + v_p K^p \quad (14)$$

where $\alpha = 2a_k/d_n$ is dimensionless parameter accounting for the thermal interfacial resistance characterized by Kaptiza radius, $a_k = R_k K^p$; in which d_n and R_k are the CNT diameter and thermal interfacial resistance of CNT/polymer while the subscripts v_n and v_p represent CNTs and polymer material volume fractions of RVE of the PMNC, respectively. Having found the $[K^{nc}]$, the next step is estimating the conductivities of HCF surrounded by PMNC material. To carry out the estimates, eqs. (11) and (12) have been considered. Once this is done, the final step towards the computation of conductivities of FFHE is achieved by considering the matrix material as the PMNC and the reinforcements as HCF. The MOC is then adopted in the final step prediction of FFHE thermal properties effectively.

Results and discussion

This section is devoted for the calculations of results obtained from the micromechanics methods proposed in the previous sections. For the validity of the proposed MOC and EM approaches, the thermal property predicted by the them are compared with the existing experimental findings. Henceforth, the same approaches have been adopted in the estimation of FFHE thermal conductivities.

Comparisons with the experimental results: The results of the experiments pertaining to conductivities in axial and transverse direction of fabricated multi-walled nanocomposite by Marconnet *et al.*³⁴ serves as the reference and the same have been predicted with the present proposed approaches. The predicted values are found to be consistent with the experimental work Marconnet *et al.*³⁴ and the same have been displayed in Figs. 6(a) and 6(b). Also, from these plots the curve best fits with experimental results are those predicted by the EM approach. The differences in the predictions made by the present approaches with the experimental ones may be attributed to the alignment factor ($AF = 1$) while the same has a value 0.77³⁴. Also, consideration of no thermal interfacial resistance between CNT/polymer¹⁵⁻¹⁸ and consideration of no defects in the CNT polymer interactions^{33,34} may be the other facts leading to this deviation. The present study considers only the thermal interfacial resistance effect of CNT/polymer on the thermal conductivity estimations since this play a vital role in significantly contributing to the same. Consideration of other factors in the study is beyond the scope of the work. Thus we can conclude to a great deal of accu-

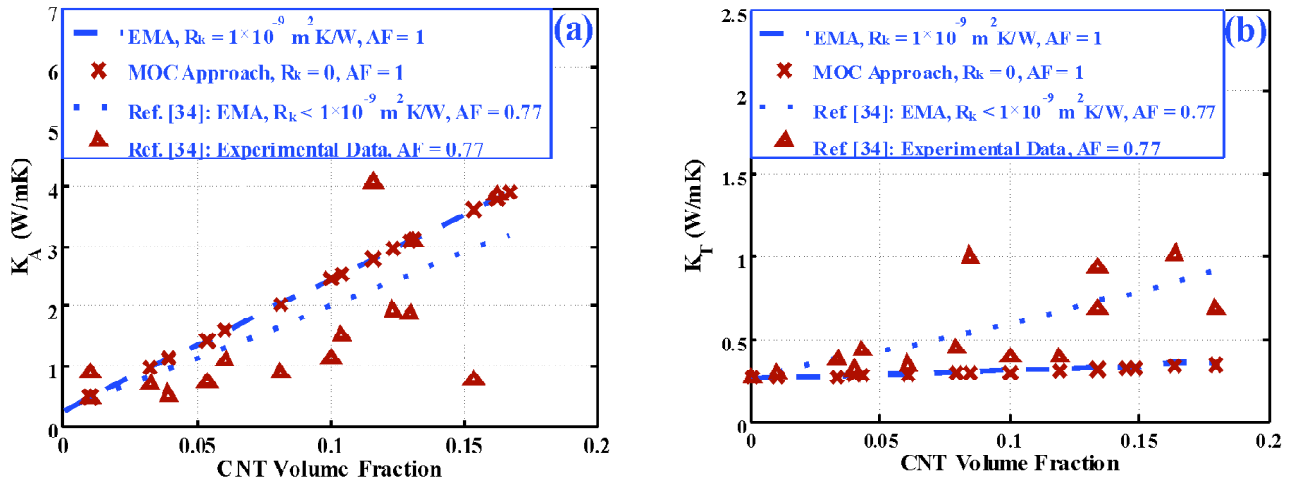


Fig. 6. Thermal conductivity comparisons of the Marconnet *et al.*³⁴ material predicted using the present micromechanics approaches with those of experimental findings of Marconnet *et al.*³⁴: (a) axial alignment (K_A) and (b) transverse alignment (K_T).

racy that the present approaches namely MOC and EM can be adopted for the estimations of conductivities of FFHE.

Analytical modeling results:

Considering the materials namely the CNT with (10, 10) armchair single-walled configuration and the polymer matrix the numerical findings are presented. Taking the HCF thermal conductivity as 35.1 W/mK (Torayca-T800H)³⁵ and the same for (10, 10) CNT (armchair) and polymer matrix being a temperature dependent function. The sought temperature range is 100–400 K for the analysis while the corresponding thermal conductivity values are 3.8×10^4 – 3.1×10^3 W/mK⁶ for CNT and 0.16–0.205 W/mK for the polymer³⁶, respectively. The temperature relationships for the CNT and the polymer are as follows^{6,36}:

$$\begin{aligned}
 K^n = & -2.3476 \times 10^{-18} T^{10} + 5.1847 \times 10^{-15} T^9 \\
 & -4.9368 \times 10^{-12} T^8 + 2.6466 \times 10^{-9} T^7 \\
 & -8.744 \times 10^{-7} T^6 + 1.8296 \times 10^{-4} T^5 \\
 & -0.02398 T^4 + 1.8888 T^3 - 85.366 T^2 \\
 & + 2256.4 T \text{ W/mK}
 \end{aligned} \tag{14}$$

$$\begin{aligned}
 K^p = & -1.2805 \times 10^{-15} T^6 + 1.8231 \times 10^{-12} T^5 \\
 & -1.0343 \times 10^{-9} T^4 + 2.9748 \times 10^{-7} T^3 \\
 & -4.6272 \times 10^{-5} T^2 - 0.0040278 T \text{ W/mK}
 \end{aligned} \tag{15}$$

The fixed dimensions of HCF containing no CNTs are inner diameter $d_i = 50 \mu\text{m}$ and outer $d_o = 100 \mu\text{m}$, respectively. Since the CNTs are on the HCFs periphery limiting its vol-

ume fraction. Hence, finding the limiting volume fraction of CNT is vital for the present analysis. Hence, to determine this, the constraint imposed is fixing the adjacent CNTs root surface distance to 1.7 nm ²⁷ with CNT diameter (d_n) and the HCF outer diameter (d) in the FFHE. The volumes V^F , V^{PMNC} and V^{FFHE} of the HCF, the PMNC and the FFHE based on the Fig. 2 are given below:

$$V^F = \frac{\pi}{4} (d^2 - d_i^2) L \tag{16}$$

$$V^{\text{PMNC}} = \frac{\pi}{4} (d_0^2 - d^2) L \tag{17}$$

$$V^{\text{FFHE}} = \frac{\pi}{4} (d_0^2 - d_i^2) L \tag{18}$$

Making use of eqs. (16) and (18), the HCF volume fraction (v_f) in respect of FFHE is given as:

$$v_f = \frac{V^F}{V^{\text{FFHE}}} = \frac{(d^2 - d_i^2)}{(d_0^2 - d_i^2)} \tag{19}$$

The constraint limitation of surface root distance of CNTs limits the quantity of CNTs (N_{CNT})_{max} presence on the outer periphery of HCF and hence the volume of CNTs (V^{CNT}) are given as

$$(N_{\text{CNT}})_{\text{max}} = \frac{\pi d L}{(d_n + 1.7)^2} \tag{20}$$

$$V_{CNT} = \frac{\pi}{8} d_n^2 (d_o - d) (N_{CNT})_{max} \quad (21)$$

Thus CNTs volume fraction limit $(V_{CNT})_{max}$ relative to the FFHE volume is as follows:

$$(V_{CNT})_{max} = \frac{V_{CNT}}{V_{FFHE}} = \frac{d_n^2 (d_o - d)}{2(d_o^2 - d_i^2)L} (N_{CNT})_{max} \quad (22)$$

While maximum limiting CNT volume fraction in reference to the PMNC $(v_n)_{max}$ is found in terms of $(V_{CNT})_{max}$ as:

$$(v_n)_{max} = \frac{V_{CNT}}{V_{PMNC}} = \frac{(d_o^2 - d_i^2)}{(d_o^2 - d^2)} (V_{CNT})_{max} \quad (23)$$

The micromechanics models used in the earlier section have also been adopted in the computation HCF thermal conductivities surrounded by the PMNC material. To make such computations, the presence of no thermal interfacial resistance (i.e. $R_k = 0$) of CNT/polymer is assumed throughout the analysis. From eq. (23) it is evident that $(v_n)_{max}$ is dependent on CNT volume fraction in the PMNC while the PMNC in itself changes with the HCF volume fraction of FFHE. Eq. (23) is hence used to predict the PMNC material thermal conductivities and the corresponding illustrations are displayed in Figs. 7(a) and (b). The figures depict that both the conductivities (K_1^{PMNC}) and (K_2^{PMNC}) in axial and transverse directions increases with the CNT volume fraction in the PMNC reaching a peak at $(v_n)_{max}$ 0.1164 for diameter of HCF $d = 60 \mu m$. Also, these results reveal that for both the tem-

peratures, the micromechanics models MOC and EM approach are in unison with each other. The cause of this unison is the perfect alignment of CNTs in the PMNC (i.e. $AF = 1$) with ($R_k = 0$). Owing to the transverse isotropic nature of the PMNC material about 1-axis, the conductivities (K_3^{PMNC}) should be identical with the values of (K_2^{PMNC}) and the results so produced have corroborated the same and for the sake of brevity are not presented here. The transverse isotropic nature of the PMNC has been well established by both the micromechanics approaches (EM and MOC), and hence any of these approaches may be adopted for predicting the FFHE properties. The MOC approach is used to study the effect of CNTs on the periphery of the HCF in the estimation of the same. For such study, the following are the values considered $d = 60 \mu m$, $T = 200 K$ and $T = 400 K$. Also, it will be important to observe the effect of change in volume fraction of the CNT in the FFHE for a fixed temperature for different values of d of the HCF. Hence, the above study is carried out for the following values of 'd' taken between ($60 \mu m$ to $90 \mu m$) and the findings are presented in Figs. 8(a) and (b). The figures show the thermal conductivity variation with temperature in both axial (K_1) and transverse direction (K_2) of the FFHE. From Fig. 8(a) it may be noted that the CNTs on the HCF has least or zero effect on FFHE thermal conductivity K_1 (axial direction). On the other hand, observing Fig. 8(b) it is seen that the value of FFHE thermal conductivity K_2 (transverse direction) decreases with the rise in the tempera-

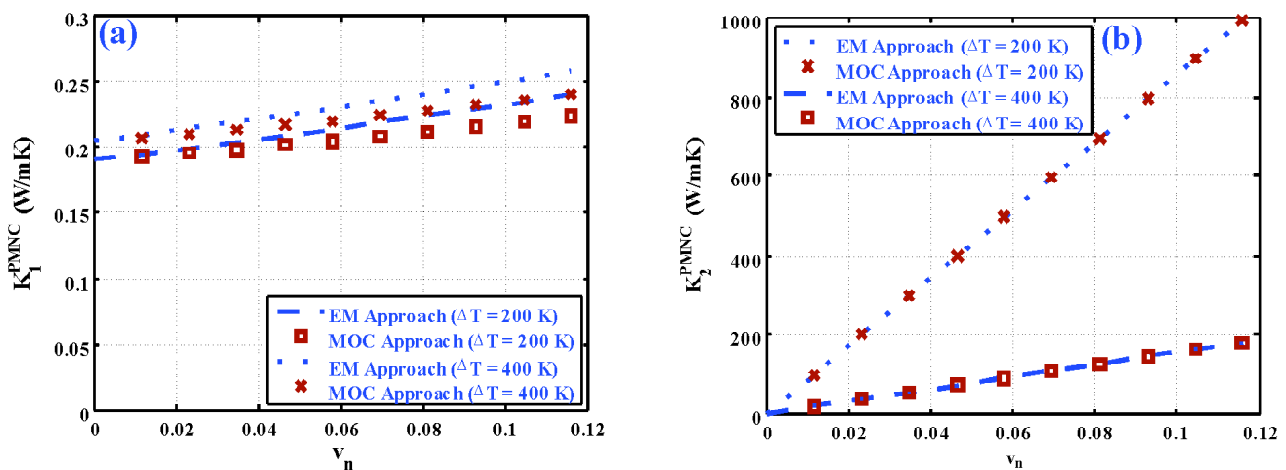


Fig. 7. PMNC thermal conductivity variation for $R_k = 0$ with V_{CNT} (volume fraction of CNT) in PMNC: (a) axial (K_1^{PMNC}) and (b) transverse (K_2^{PMNC}).

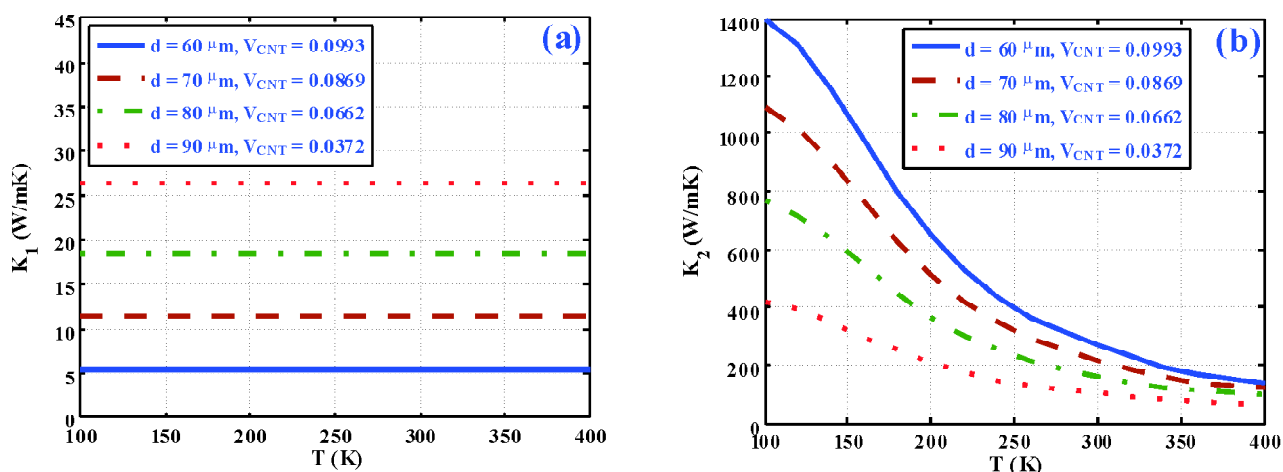


Fig. 8. Effective thermal conductivity variation of FFHE for zero thermal interfacial resistance ($R_k = 0$): (a) axial (K_1) and (b) transverse (K_2) with the temperature.

ture. The reason for this behavior of K_2 is based on the fact that the significant decrease in K^n with rise in temperature of the straight grown radial CNTs on the periphery of the HCF. It is also motivating to note that for the CNT volume fraction 9.93% in FFHE and $d = 60 \mu\text{m}$, significant enhancements in the values K_2 of FFHE over the HCF with no CNTs is observed and the corresponding enhancements are 661% and 293% for the temperatures of 300 K and 400 K. This shows that CNTs presence on HCF augments the out-of-plane PMNC conductivities. The other thermal conductivity K_3 estimated with the procedure mentioned above are found to be in unison with the values of K_2 and hence for brevity sake they are not displayed here. The match in these values establishes the 1-axis transverse isotropy nature of the FFHE. The analysis carried out so far did not account for CNT/polymer thermal interfacial resistance (i.e. $R_k = 0$). However, considering the same may affect the thermal properties whereby resulting in the performance reduction of the FFHE. Therefore, to assess this effect, R_k values of CNT/polymer is varied till $20 \times 10^{-8} \text{ m}^2\text{K/W}$ ^{13,14}. Fig. 9 illustrates this consequence K_1^{PMNC} (thermal conductivity) of the PMNC for $T = 400 \text{ K}$. From the figure it is seen that K_1^{PMNC} falls swiftly with rise in R_k till $3 \times 10^{-8} \text{ m}^2\text{K/W}$ beyond which the same K_1^{PMNC} stabilizes becoming asymptotic. Similar results of not presented here have been observed in the estimates K_2^{PMNC} , K_3^{PMNC} , K_1 , K_2 and K_3 .

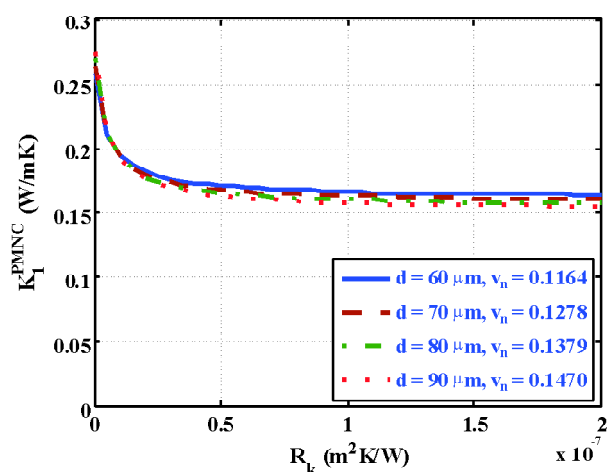


Fig. 9. Thermal conductivity (K_1^{PMNC}) variation in axial direction of the PMNC with thermal interfacial resistance (R_k) CNT/polymer ($T = 400 \text{ K}$).

Conclusions

Carbon fuzzy fiber heat exchanger (FFHE) is a novel concept that is being proposed in the current study. The three materials which make up the FFHE a novel idea are the base hollow carbon fiber (HCF), the polymer matrix (PM) and the carbon nanotubes (CNTs). Micromechanics based approaches like the MOC and EM have been employed to predict the carbon FFHE thermal conductivities. The summary and findings of the present study are:

The straight CNTs that are grown radially on the periph-

ery of the HCF significantly enhances FFHE thermal conductivities in the transverse direction in comparison with those of a HCF with no CNTs.

However, the same effect of significant enhancement of the thermal property is not seen in the axial direction and in fact a decrease in the same has been observed with presence of CNTs on the HCF.

The study also corroborates the fact that the consideration of thermal interfacial resistance (CNT/polymer) has negligible or zero effect on the final predicted FFHE thermal properties.

The significant enhancement in transverse conductivities ensure the fact that suitability of FFHE as heat exchanger for miniature electronics and semiconductor applications. Also, the present findings certainly brings an insight to the future researchers in performing the analysis for closer estimates with that of experimental results.

References

1. S. Iijima, *Nature*, 1991, **354**, 56.
2. M. M. J. Treacy, T. W. Ebbesen and J. M. Gibson, *Nature*, 1996, **381**, 678.
3. C. Li and T. W. Chou, *Int. J. Solids Struct*, 2003, **40(10)**, 2487.
4. L. Shen and J. Li, *Phys. Rev. B*, 2004, **69(4)**, p. 045414.
5. J. Hone, M. Whitney, C. Piskoti and A. Zettl, *Phys. Rev. B*, 1999, **59(4)**, 2514.
6. S. Berber Y. K. Kwon and D. Tomaneck, *Phys. Rev. Lett.*, 2000, **84(20)**, 4613.
7. J. R. Lukes and H. Zhong, *J. Heat Trans-TASME*, 2007, **129**, 705.
8. L. Wei, F. Yanhui, P. Jia and Z. Xinxin, *J. Heat Trans-TASME*, 2012, **134**, 092401.
9. S. U. S. Choi, Z. G. Zhang, F. E. Lockwood and E. A. Grulke, *Appl. Phys. Lett.*, 2001, **79(14)**, 2252.
10. M. J. Biercuk, M. C. Llaguno, M. Radosavljevic, J. K. Hyun and A. T. Johnson, *Appl. Phys. Lett.*, 2002, **80(15)**, 2767.
11. C. Guthy, F. Du, S. Brand, K. I. Winey and J. E. Fischer, *J. Heat Trans.-TASME*, 2007, **129**, 1096.
12. C. W. Nan, Z. Shi and Y. Lin, *Chem. Phys. Lett.*, 2003, **375**, 666.
13. O. M. Wilson, X. Hu, D. G. Cahill and P. V. Braun, *Phys. Rev. B*, 2002, **66(22)**, p. 224301.
14. S. T. Huxtable, D. G. Cahill, S. Shenogin, L. Xue, R. Ozisik, P. Barone, M. Usrey, M. S. Strano, G. Siddons, M. Shim and P. Keblinski, *Nat. Mater.*, 2003, **2(11)**, 731.
15. C. W. Nan, G. Liu, Y. Lin and M. Lin, *Appl. Phys. Lett.*, 2004, **86(16)**, 3549.
16. M. B. Bryning, D. E. Milkie, M. F. Islam, J. M. Kikkawa and A. G. Yodh, *Appl. Phys. Lett.*, 2005, **87**, p. 161909.
17. Q. Z. Xue, *Nanotechnology*, 2006, **17(6)**, 1655.
18. A. S. Cherkasova and J. W. Shan, *J. Heat Trans.-TASME*, 2010, **132**, 082402.
19. S. Maruyama and R. Xiang, *J. Heat Trans.-TASME*, 2012, **134**, p. 051024.
20. C. Bower, W. Zhu, S. Jin and O. Zhou, *Appl. Phys. Lett.*, 2000, **77(6)**, 830.
21. E. T. Thostenson, W. Z. Li, D. Z. Wang and T. W. Chou, *Appl. Phys. Lett.*, 2002, **91(9)**, 6034.
22. Z. G. Zhao, L. J. Ci, H. M. Cheng and J. B. Bai, *Carbon*, 2005, **43**, 651.
23. V. P. Veedu, A. Cao, X. Li, K. Ma, C. Soldano, S. Kar, P. M. Ajayan and M. N. Ghasemi-Nejhad, *Nat. Mater.*, 2006, **5**, 457.
24. E. Bekyarova, E. T. Thostenson, A. Yu, H. Kim, J. Gao, J. Tang, H. T. Hahn, T. W. Chou, M. E. Itkis and R. C. Haddon, *Langmuir*, 2007, **23(7)**, 3970.
25. N. Yamamoto, S. S. Wicks, R. Guzman de Villoria, K. Ishiguro, S. A. Steiner III, E. J. Garcia and B. L. Wardle, 17th ICCM, Edinburgh, Scotland, 2009, July 27-31.
26. J. Chen, X. Xiong and P. Xiao, *Mater. Chem. Phys.*, 2009, **116(1)**, 57.
27. S. I. Kundalwal and M. C. Ray, *Int. J. of Mech. Mater. Des.*, 2011, **7(2)**, 149.
28. G. Chatzigeorgiou, G. D. Seidel and D. C. Lagoudas, *Compos. Part B-Eng.*, 2012, **43(6)**, 2577.
29. J. Aboudi, S. M. Arnold and B. A. Bednarczyk, <https://doi.org/10.1016/C2011-0-05224-9>. Butterworth-Heinemann Ltd., Oxford OX5, UK, 2013.
30. H. Hatta and M. Taya, *J. Appl. Phys.*, 1985, **58(7)**, 2478.
31. S. C. Cowin and M. Fraldi, *Int. J. Nonlin Mech.*, 2005, **40**, 361.
32. C. W. Nan, R. Birringer, D. R. Clarke and H. Gleiter, *J. Appl. Phys.*, 1997, **81(10)**, 6692.
33. A. Yu, M. E. Itkis, E. Bekyarova and R. C. Haddon, *Appl. Phys. Lett.*, 2006, **89**, 133102.
34. A. M. Marconnet, N. Yamamoto, M. A. Panzer, B. L. Wardle and K. E. Goodson, *ACS Nano*, 2011, **5(6)**, 4841.
35. TORAYCA. *Technical Data Sheet No. CFA-007*, Inc., 6 Hutton Centre Drive, Santa Ana, CA. See also URL <http://www.toraycfa.com/pdfs/T800HDataSheet.pdf>.
36. W. Reese, *J. Appl. Phys.*, 1996, **37(2)**, 864.